Noninvasive Tracking of Gene Transcript and Neuroprotection after Gene Therapy

HHS Public Access

Author manuscript

Gene Ther. Author manuscript; available in PMC 2016 May 18.

Published in final edited form as:

Gene Ther. 2016 January ; 23(1): 1–9. doi:10.1038/gt.2015.81.

Noninvasive Tracking of Gene Transcript and Neuroprotection after Gene Therapy

Jiaqian Ren[1], **Y. Iris Chen**[1], **Christina H. Liu**[1], **Po-Chih Chen**[2], **Howard Prentice**[2], **Jang-Yen Wu**[2], and **Philip K. Liu**[1,*]

[1]Athinoula A. Martinos Center for Biomedical Imaging, Department of Radiology, Massachusetts General Hospital and the Harvard Medical School, Charlestown, MA

[2]Department of Biomedical Science, Charles E. Schmidt College of Medicine, Florida Atlantic University, Boca Raton, FL

Abstract

Gene therapy holds exceptional potential for translational medicine by improving the products of defective genes in diseases and/or providing necessary biologics from endogenous sources during recovery processes. However, validating methods for the delivery, distribution and expression of the exogenous genes from such therapy can generally not be applicable to monitor effects over the long term because they are invasive. We report here that human granulocyte colony-stimulating factor (hG-CSF) cDNA encoded in scAAV-type 2 adeno-associated virus, as delivered through eye drops at multiple time points after cerebral ischemia using bilateral carotid occlusion for 60 min (BCAO-60) led to significant reduction in mortality rates, cerebral atrophy, and neurological deficits in C57black6 mice. Most importantly, we validated hG-CSF cDNA expression using translatable magnetic resonance imaging (MRI) in living brains. This noninvasive approach for monitoring exogenous gene expression in the brains has potential for great impact in the area of experimental gene therapy in animal models of heart attack, stroke, Alzheimer's dementia, Parkinson's disorder and amyotrophic lateral sclerosis, and the translation of such techniques to emergency medicine.

Keywords

biologic; cardiac arrest; forebrain ischemia; G-CSF; hypothermia; neurogenesis; targeted- delivery

Introduction

Alzheimer's dementia (AD), an age and genetic-related disorder, affects 4.5 million Americans. The risk to develop AD and stroke can be associated in elderly people[1], and a common pathway (p25.cdk5) leads to elevated production of amyloid protein beta in

*Address correspondence to: Philip K. Liu, Ph.D., CNY149 13th Street, Charlestown, MA 02129-2020, ; Email: philipl@nmr.mgh.harvard.edu, (617) 724-4563

Conflict of Interests: The authors declare no competing financial interests.

individuals with stroke and AD[2]. The granulocyte-colony stimulating factor (G-CSF) in patients diagnosed with AD is found to be significantly lower than age-matched people[3]. G-CSF is a cytokine that stimulates growth and differentiation of myeloid precursors[4]. The expression of G-CSF and its receptor in the microvessels of the CNS suggests that G-CSF provides autocrine neuroprotection in response to brain damage[5]. In pre-clinical tests, G-CSF has been shown to pass through the blood-brain barrier by receptor-mediated endocytosis, leading to a reduction in infarct volume in rat models of acute stroke[6]; G-CSF reduces the level of beta amyloid deposited in excess in the brain and reverses memory impairment in mice genetically altered to develop AD[7]. In addition, studies in different animal models of stroke, Parkinson's disease, and other neurodegenerative disorders have specifically demonstrated that G-CSF may protect neurons, increase blood vessel growth, and improve motor function[8–10]. A phase IIb trial has also tested the safety of G-CSF[11]. On the other hand, a recent clinical study demonstrated that direct injection of exogenous G-CSF protein to the vasculature of 328 acute stroke patients showed a trend to reduce infarct growth, but did not reduce mortality, infarct size or neurological score[12]. The discrepancies between clinical and preclinical responses can partially arise from different approaches used to validate the delivery of exogenous biologics and examine the molecular basis of their therapeutic effects are primarily histology based. These histological methods have limited benefit because they rely on the use of invasive tissue sampling and, because they involve the removal of the very tissue we wish to protect, preclude long-term monitoring. To overcome these limitations we need to re-evaluate the responses using a noninvasive approach to monitor the delivery, expression of exogenous G-CSF genes and its efficacies in the central nervous system of living conditions[1314].

We tested the hypothesis that a neuroprotective biologic encoded in the cDNA carried by a viral vector could be delivered at multiple time points using eye drops to forebrain ischemia model using BCAO-60 in C57blcak6 mice[14–16]. BCAO-60 does not induce significant infarct, although DNA and brain damage can be repaired[17]. By encoding human G-CSF (hG-CSF) in a replication-deficient, self-complementary adeno-associated virus (AAV) vector (scAAV2-CMV-hG-CSF) it may be possible to elicit a continuous supply of endogenous G-CSF[18]. The use of the AAV2 vector, with optimally selected serotype, has proved highly valuable for efficient transduction in the CNS, and for rapid initiation of expression[19]. For example, AAV2 vectors carrying exogenous genes have been employed to examine transduction in brain tissue in vivo in models of AD, amyotrophic lateral sclerosis and Parkinson's disease[16,20,21].

Most significantly, we have developed two noninvasive measurements as alternatives to invasive biopsy procedures. First, we developed MR contrast agents (MR-CAs) to target unique mRNA expression of hG-CSF cDNA in the brains of living mice without biopsy. Second, we established and validated measurements to noninvasively monitor neuroprotection after gene therapy, so that these responses are consistent with hypothermia treatment (34°C, whole-body) during cerebral ischemia, a therapeutic method that has been shown to reduce brain injury after cardiac arrest and traumatic brain injury[22–24]. We demonstrate this approach as an alternative to destructive sampling methods. Such assays would allow long-term monitoring of neuroprotection and continuous expression of exogenous cDNA, as gene therapy becomes translatable to clinical applications. This

monitoring system will be central to evaluating the therapeutic efficacy of exogenous cDNA in the CNS.

Results

We first characterized noninvasive measurements of cerebral damage in C57black6 mice. In C57black6 mice, BCAO-60 induces global oxidative stress, DNA damage, apoptosis, but very limited infarction in the brain[14,15,25,26]. Figure 1*a* shows the protocol used for BCAO induction and longitudinal monitoring. This cerebral ischemia model is associated with severe weight loss (Fig. 2) and a mortality rate of 75 ± 10% within the first week. In common with other animal models of cardiac arrest or stroke[27–29], we have reported that BCAO-60 induces regional abnormal water movement (edema), as evidenced by enhanced diffusion-weighted imaging (hDWI), within the first two days (Fig 1*b1*); the regions with hDWI were localized in the forebrain and midbrain (Fig. 3). To overcome the lack of measurable infarct in this BCAO model, we translated the increased hDWI to the reduced apparent diffusion coefficient (rADC), and we quantitatively measured the regions with significant rADC in the brain before and one day after BCAO-60 (Fig 1*b2*). We found VMD is characteristically bi-phasic with a second peak appearing at >10 hours, and the second peak became stable at one to 2 days with pseudo normalization toward the values before cerebral ischemia in the striatum (Fig. 4). We measured DWI and VDM thereafter at one day after BCAO-60 (Fig 3). Without effective treatment, the brains would develop cerebral atrophy and eventual ventriculomegaly by the 4th week (Fig 1*c1*). Indeed, we found that lateral ventricular size (LVS) increased to 4.3% post BCAO-60 significantly ($p = 0.01$, Student *t* test, one tail) from 2.1% in sham-operated mice (Fig. 1*c2*); atrophy measured at 4 weeks and beyond positively correlated with the estimated VMD at one day in living mice post BCAO-60, with a linear coefficient of 0.71.

Unlike mice with brain damage, when normal animals encounter a corner they typically rear forward and upward, then turn back, in either direction, to face away from the corner and toward the open end of the setup (the corner test)[30,31]. We measured the rate of turns when normal mice faced a 30° corner (i.e., turning to either the left or right) to have a rate of 50 ± 8% (symmetric and no bias) before BCAO-60. Mice were measured weekly for at least four weeks after the BCAO-60 procedure (Fig 1*d*). We observed a significant increase in asymmetric turning (~90% to one side) in BCAO-60 mice.

To validate ventriculomegaly and corner tests as robust indicators of the severity of brain damage and treatment responses, we randomly treated a group of the BCAO-60 mice with whole-body hypothermia, whereby the animals were placed on ice immediately after vessel occlusion and returned to room temperature when rectal body temperature measured 34°C during the 60-minute procedure (hypothermia group). Hypothermia treatment was found to significantly improve survival, from 25 ± 10% to 100%, in this group. We found hypothermia significantly reduced lesions and cerebral atrophy in the striatum and cortex (Fig. 1*e* & 1*f*). Furthermore, we found that this neuroprotection involved a reduction in the expression of MMP-9 (Fig. 1*g1* & 1*g2*). Hypothermia therapy was also associated with a significant reduction in asymmetric turning, from 0.9 to 0.58 ($p<0.05$), a rate not significantly different from that seen in the sham operation group; these results were

consistent throughout the 4 weeks of weekly tests following BCAO (Fig. 1*d*). Our data thus demonstrated that ventriculomegaly and performance in the corner test served as accurate indicators of the severity of brain damage in this BCAO model.

Genes carried by an AAV vector are delivered as one single-bolus dose in most gene therapies. To evaluate gene therapy using eye drop delivery, we administered a single dose of scAAV2-CMV-hG-CSF (3×10^9 pfu; 1.5 μl to the conjunctival sac of the left eye) at 0.5 (n = 9), 1, 2, 3, 4, or 24 hours (n = 3, each group) after the release of BCAO. Survival rate varied depending on the time of eye drop administration (i.e., 78% for the 0.5 hr group, 66% for the 1 and 3 hr groups, 33% for the 4 hr group and 100% for the 2 and 24 hr groups), but in each instance it was greater than the ~25% survival seen in the group treated with scAAV2-CMV-GFP similarly administered (placebo, n = 15). Moreover, there was no significant reduction in ventriculomegaly compared to the group received scAAV2-CMV-GFP (Fig 5*a*).

When we applied additional scAAV2-CMV-hG-CSF at 0.5 hr, 1, 7 and 14 days after BCAO-60 (n = 7), we observed an exceptionally high survival rate of 100%, compared to ~25% in the BCAO-60 without treatment group (n = 22). The optimal window for multiple scAAV2-CMV-hG-CSF treatments after BCAO coincides with the development of bi-phasic VMD (Fig 4). More importantly, we found that multiple doses of scAAV2-CMV-hG-CSF significantly reduced cerebral atrophy (Fig. 5*a*). Gene therapies with hG-CSF cDNA ameliorated asymmetric turning in the corner test, from 0.9 in the placebo mice (BCAO with scAAV2-CMV-GFP, placebo group) to 0.67 ± 0.1 (Student *t* test, p=0.03, one tail, n ≥ 5 each group), a result not significantly different from that measured before BCAO, i.e., 0.50 ± 0.08. We did not compare the corner tests in single dose groups because variable surviving mice.

To demonstrate positive hG-CSF mRNA expression in vivo, we designed a phosphorothioate-modified oligo DNA with antisense sequence (AS) hG-CSF and Cy3 label (sODN-AS-hG-CSF-Cy3). After transfecting PC-12 cells with scAAV2-CMV-hG-CSF or scAAV2-CMV-GFP DNA we found PC-12 cells expressed exogenous hG-CSF mRNA 6 hours after transfecting using real-time cell imaging for Cy3 or DNA-free RT-PCR (Fig. 6*a* & 6*c*); no hG-SCF mRNA expression was found in the placebo group at any of the time points tested (Fig. 6*b*–6*c*). We successfully showed that secondary GFP^+ transfectants using DNA extracted from primary transfectants of the placebo group exhibit real-time expression of GFP (Fig. 6d & 6e); these data supported a stable scAAV2 vector and its cDNA after gene therapy. Moreover, these data indicate that the sequence in the sODN-AS-hG-CSF-Cy3 will distinguish hG-CSF mRNA from the endogenous rodent mRNA.

We found that hG-CSF mRNA expression was clearly represented as unique ROIs in the R2* map when SPION-AS-hG-CSF and MRI were acquired 3 to 4 weeks after BCAO (arrows, Fig. 5*b1*). However, we observed some enhanced ROIs in the placebo group (Fig. 5*b2*); such noise was mainly near the injured site surrounding the ventricle with ventriculomegaly (asterisk). We used data from target-guided MRI to obtain tissue sample and validated hG-CSF antigen expression to be localized in the non-astroglial population (Fig. 5*c*); the expression of hG-CSF in the placebo group was negligible (Fig 5*d*). We showed that NeuN expressed in most small blood vessels in mice treated with scAAV2-

CMV-hG-CSF (arrow, Figure 5*e*); in the control groups (no virus treatment or placebo) the expression of NeuN was found mostly in the nucleus.

To demonstrate the route of scAAV2-CMV-hGCSF or -GFP distribution after eye drop administration, we applied non-targeting Gd-DTPA to the right conjunctival sac (n = 4). Compared to pre-existing signal in fatty tissue (Fig 5f), we noticed a conspicuous elevation of R1 signal in the ipsilateral bulbar and palpebral conjunctiva (ROI near the lens, as denoted by the asterisk) as well as in the naso-lacrimal canal (arrow) 5–10 minutes after application (center panel, Fig 5*f*); enhanced MR-CA distribution becomes apparent in the naso-lacrimal canal on the contralateral side at 30 minutes. We found no MR-CA in the lens and cornea (asterisk), regions where lymphatics are lacking. We then tested the route of distribution after eye drop application in mice (n =3, 14 days after BCAO-60) using targeting Gd-NA-nestin (1 μg Gd-DTPA in 2 μl). This targeting MR-CA binds to nestin mRNA of pericytes in the neovasculature when intraperitoneally injected to mice after BCAO-60[14,15]; we acquired longitudinal MRI (Figs 5g1–5g4). Figure 5g shows enhanced R1 signal in the brain three hours after eye drop application (asterisks, Fig 5g1 vs. Fig 5g3); in addition, we noticed R1 signal in the brain (asterisks) and retina (arrows) where the blood-retina barrier in the choroid might become permeable to MR-CA following BCAO-60. The data we have acquired support the hypothesis that viral vectors for treatment of BCAO-induced brain injuries can be distributed via the orbital lymphatics after delivery through eye drops applied to the conjunctival sac.

Discussion

To the best of our knowledge in the area of theragnostics using gene therapy, this study is the first of its kind to demonstrate effective noninvasive delivery of hG-CSF cDNA in scAAV-type 2 adeno-associated virus via eye drops, and to examine hG-CSF mRNA expression from neural cells in living mouse brains without biopsy. Furthermore, this study is distinct in that it tracked the neurological and histological effects of gene therapy for acute cerebral ischemia. Expression of the exogenous hG-CSF cDNA carried by scAAV2-CMV-hG-CSF and delivered through the eye conjunctiva are found to be effective in reversing neurological symptoms (the corner test) and ventriculomegaly in the brain after ischemia. These data lead us to conclude that repeated administration of hG-CSF cDNA in scAAV-type 2 adeno-associated viruses can protect the brain by supplying endogenous biologic of hG-CSF from neural cells during critical time after BCAO-60, leading to reductions in mortality, cerebral atrophy and the neurological deficits associated with ischemia. In mice that undergo brain repair using gene therapy is mediated by the elevation of neural progenitor cells in the small blood vessels. None of the improvements noted above were observed in mice of the placebo group. We validated noninvasive measurements used in our studies by comparing the results after hypothermia treatment. In normal mice, hypothermia may elevate DWI and reduce ADC. However, we measured rADC one day after hypothermia. Even so the rADC by hypothermia in normal micecould inflate lesion estimation based on the threshold ADC and overestimated the VMD in this hypothermia group (Fig 1*g*). Even so, The finding that hypothermia significantly reduces VMD induces less MMP-9 after BCAO-60 is consistent with our previous using MMP-9 gene knockdown in normal temperature[32].

Single doses delivered at various time points within the first 24 hours after injury are found to be less effective in reversing brain damage. Our results from a single application of scAAV2-CMV-hG-CSF confirm the less-than-optimal effect of single-dose delivery of murine G-CSF cDNA in scAAV1/2 to the mouse spinal cord[16]. It is also important to note that for our BCAO model there may be a window immediately after release of vessel occlusion during which uptake and distribution of hG-CSF cDNA are variable. The variability in the reduction of ADC most likely represents the change in the severity of hDWI, elevated MMP-9 expression and/or defective BBB. Therefore, the change in rADC at the second peak supports our rationale to deliver multiple doses of hG-CSF cDNA in scAAV-type 2 adeno-associated viruses. Cerebral damage and disturbance of the BBB were demonstrated by variations in the ADC threshold, which was previously established using power analysis in a project involving 52 normal mice that underwent BCAO at normal temperature[32]. The association of brain damage to the location of lesions with below-threshold ADC was supported by MMP-9 expression (Fig 1*h*); this association is validated by studies, from two different investigators, that used a global ischemia model with potassium chloride and resuscitation[27,28].

The damage that occurs in the brain in the first few hours after cerebral ischemia may reflect reperfusion, and thus exhibit as “normalization” toward the baseline ADC, followed by another elevation of VMD in the secondary ADC drop that continues for at least 48 hours. The lower lesion severity between 3 and 7 hours after BCAO may explain the less-than-optimal efficacy of scAAV2-CMV-hG-CSF treatment we observed at 4 hours. Therefore, although a single dose of scAAV2-CMV-hG-CSF on day one was found to improve survival rate, it did not reduce either cell death or neurological deficits. Indeed, repeated applications of scAAV2-CMV-hG-CSF after the initial 4-hour time point ensure continuous supplies of hG-CSF in our studies. Increased blood vessel growth has been demonstrated in mice treated with G-CSF protein by showing greater numbers of bone marrow neural precursor cells in the vessels[33,34], and we demonstrated the same after repeated treatment. This result suggests that hG-CSF must be present during reperfusion and for at least 7 days for edema-related brain damage and neural cell death to be reversed[35].

We propose that the viral vector is transported through the lymphatic fluid (Fig 5*f–g*) to the vena cava, and then through the blood circulation to the brain, reaching the perivascular space by way of the BBB damaged as a result of cerebral ischemia[14,15]. After the viral particles reach the perivascular space, they may be transported across the cell membrane for intracellular expression[36]. Another distribution route of the viral vector can be via the blood-retina barrier, which will need a retina-specific MR-CA for future evaluation.

Our findings support the hypothesis that G-CSF reduces neurological deficits that develop in the first few days after cerebral ischemia. The corner test is one of more than five sensorimotor tests (including forelimb flexion, forelimb placing, accelerated roared and adhesive removal tests) used to assess neurological deficits in rodents. Among these tests, the corner test is regarded as “more sensitive” in detecting deficits than the other tests because it reflects multiple asymmetries, including forelimb, hind limb, postural and turning bias[37]. It has been established for mice affected by focal cerebral ischemia induced by the middle cerebral artery occlusion model; infract volume is correlated with performance on

the corner test for chronic behavioral impairments even as many as 90 days after mild focal cerebral ischemia, and whether with or without treatment[23, 38]. We confirmed here that the corner test can be used in BCAO model that does not induce infarcts. We have demonstrated here that gene delivery and resulting protection of the brain can be validated without removing the brain tissue we hope to preserve. Moreover, the ability to deliver therapeutic agents through eye drops may have important implications for emergency medicine, as lyophilized viral particles can be readily reconstituted in saline and administered to cardiac arrest patients.

Materials and Methods

Cell Culture

We examined the delivery and dynamic uptake of pCMV-hG-CSF and pCMV-GFP transfection in PC12 cells (ATCC, CRL-1721) in a miniature incubator chamber (INU-UK-F1; Tokai Hit Inc., Shizuoka, Japan) on the stage of an upright microscope (Olympus, Lebanon, NH, USA), following published procedure[39]. All cell culture studies were repeated by two separated research staffs.

Expression of hG-CSF cDNA

The scAAV2-CMV-GFP plasmid we used in our study was a gift from Dr. D. McCarty (Ohio State University, Columbus, Ohio) to Dr. JYW. hG-CSF 615 bp cDNA (accession number NM 172219.2) was inserted into the scAAV2-CMV-GFP plasmid by substituting hG-CSF for the GFP cDNA sequence. The new plasmid was thus termed scAAV2-CMV-hG-CSF. The scAAV-type 2 adeno-associated viruses, produced (two separate batches) by the Gene Therapy Vector Core of the University of North Carolina (Chapel, Hill, NC), were generously gifted to Massachusetts General Hospital for explicit research use. Viral titers were determined by dot blot analysis. To test gene expression in vivo, vectors were transiently transfected using lipofectin (Invitrogen) into PC12 cells (50 cells per well) at a total concentration of 1 μg/well in a 6-well dish. At 3, 6, 8, or 24 hours (one dish per time point) after transfection with scAAV2-CMV-hG-CSF plasmid or scAAV2-CMV-GFP plasmid PC12 cells were harvested for RNA isolation using RNA-easy (Qiagen) with the addition of RNase-free DNase before reverse transcription. We generated a primer with antisense (AS) sequence (5’-AACTCGGGGGAGATCCCTTCCA, homemade) to hG-CSF mRNA (AS-hG-CSF) and sense sequence (5”ACTCTCTGGGCATCCCCT, S-hG-CSF). A hG-CSF—specific reverse transcription product using primer AS-hG-CSF was generated using reverse transcriptase, PCR amplification and the DNA product was resolved by agarose gel (1%) electrophoresis, as described previously[40]. To analyze the duration of GFP expression following scAAV2-CMV-GFP plasmid transfection, images were collected by time-lapse optical microscopy (Olympus IX83) from living PC12 cells. A cellSens system (Olympus USA) was used to reconstruct the Z stack image from seven photos (Z dimension +8.82 micron with Z spacing = 1.26 microns; exposure time = 661 ms × 4.22 gain).

Animals and Housing

All procedures were approved by the Massachusetts General Hospital Subcommittee on Research Animal Care, in accordance with the Public Health Service Guide for the Care and

Use of Laboratory Animals. At least ten adult C57black6 male mice were ordered from Taconic Farm (Germantown, NY) each time (n ≥ 3 litters at a time), 2–3-months of age (23 ± 2 gm bw), were kept in cages in a room with controlled light cycles (12h/12 h light/dark). All animals had free access to water and standard lab chow. We conducted stratification for baseline values (MRI and corner test) to eliminate abnormal anatomical brains or bias corner test before experimentation. Mice were trained, operated on, and tested in a random manner, with a blinded observer performing all behavioral testing. A numeric identifier for each mouse and was given to the examiner; the treatment was revealed at the completion of testing for data analysis.

Bilateral Carotid Artery Occlusion (BCAO) to Induce Cerebral Ischemia

We used the BCAO model, as described, to for long-term examination of the delivery and dynamics of our therapeutic agents[41]. For each BCAO experiment, we randomly selected 6 mice each day and arbitrarily assigned them to one of three groups (sham operation control, BCAO, or BCAO plus treatment, n = 2 each). The control animals underwent surgical procedures identical to BCAO, except that we did not occlude the arteries (n = 4). For all normothermic animals (n = 22), we maintained body temperature at 36 ± 1°C using a heating blanket, and monitored temperature with a rectal thermos-sensor, throughout BCAO. We analyzed the blood flow of the mid-cerebral artery using Doppler in all animals that underwent surgical procedures, positioning the Doppler probes to the skull during BCAO (n = 4 of 20); these mice were not used for further experimentation. We randomly selected animals and placed them on ice immediately after the completion of vessel occlusion; they were immediately removed from the ice when body temperature dropped to 34°C (the hypothermia group, n = 10). The mice were then kept at room temperature for the remainder of the procedure, before release of vessel occlusion. The average body temperature in the hypothermia group was 34 ± 0.5°C. We applied ScAAV2-CMV-hG-CSF, scAAV2-CMV-GFP (3×10^9 pfu), or saline (1.5 μl) to the eye sac of the left eye after release of BCAO, at single (n = 24) or multiple (n = 7) time points, as indicated. By the third day after cerebral ischemia, all of the surviving post-ischemic mice exhibited spontaneous activity in their home cages, were responsive to handling, and engaged in normal self-grooming behavior.

MRI Protocols for Diffusion-Weighted MRI and Gene-Targeting MRI

Diffusion-Weighted MRI was performed in mice before and after BCAO following previously published procedure[32], using a 9.4 Tesla MRI system (Bruker Avance system, Bruker Biospin MRI, Inc., Billerica, MA). *Ventricular* images were acquired using a T2-weighted spin echo sequence (TR/TE=7000/25ms, $120\times120\mu m^2$ in-plane resolution and 20 slices of 0.5mm thickness, RARE factor 8, NA=4) on a 9.4T system. We segmented the ventricles from the tissue using a threshold of two standard deviations (0.3% confidence interval outside of the mean) above the mean signal intensity of the entire brain slice (including the ventricles).

We have shown T2 MRI to be correlated with volume measured by the threshold ADC[14]. However, BCAO-associated cerebral ischemia does not consistently induce necrosis, and SPION-hG-CSF delivered to measure gene expression may interfere with T2 MRI. Therefore, we applied threshold ADC (ADC values at three standard deviations below the

average of n = 6–9 at different dates, and examined different litters of mice). We identified volumes of metabolic disturbance (VMD) as brain lesions where rADC is evident in hyperintense diffusion-weighted images (hDWI) after BCAO, as previously described[32].

To detect hG-CSF cDNA expression *in vivo*, we generated a phosphorothioate-modified oligodeoxynucleotide (sODN) with antisense (AS) sequence (5'-Cy3-sODN-AS-hG-CSF-biotin-3', homemade) to hG-CSF mRNA. Genetic MR-CA was made by conjugating SPION to sODN-AS-hG-CSF at 3 nmol per mg Fe, as described[41]. We examined the expression of hG-CSF cDNA after BCAO by acquiring MR images at 15T (Magnex 130 mm diameter horizontal magnet with a Siemens clinical console) using SPION-AS-hG-CSF or SPION-Ran (4 mg Fe per kg, 0.1 ml, i.p,) injected the night before MRI. SPION was conjugated with Cy3-sODN-AS-hG-CSF or sODN-Ran at 1 mg Fe per 3 nmol sODN for at least 6 hrs before delivery, at 4°C. We measured non-specific R2* changes using non-targeting binding MR contrast agent (SPION-Ran), and evaluated SPION-labeled gene expression in the R2* maps acquired using multi-echo gradient echo sequences: TR 800ms, 6 echoes (TE = 1.94, 3.41, 4.88, 6.35, 7.82, 9.29ms) with spatial resolution of 0.1mm × 0.1mm × 0.25mm. We also obtained the ventricular volume from T2-weighted turbo spin echo images acquired at 15T (TR 3s, effective TE 42ms, Turbo factor 8). The total size of the segmented area (including both lateral ventricles, 3rd and 4th ventricles) was measured, normalized to the total area of the corresponding brain slices, and expressed as the ratio of ventricular volume to brain volume, in percentage.

Corner Tests

The corner test, which determines an animal's asymmetric direction of turning when encountering a corner, is used as an indicator of brain injury. We used an experimental corner setup composed of two boards (with dimensions of 30 × 20 × 1 cm^3) arranged to form a 30° corner; a small opening was left along the joint between the two boards. The mouse was placed 12 cm from the corner and allowed to walk into the corner, so that the vibrissae on both sides of the animal's face made contact with the two boards simultaneously. Before BCAO procedure, we conducted behavior tests (stratification) on all mice to screen for mice with no turning asymmetry ($n \geq 18$). Each mouse took part in ten trials, after which we calculated the percentage of turns to each side, recording only those turns involving full rearing along one of the boards. This stratification procedure excludes mice with 80–100% asymmetric turns (n=4); we included mice that turned in either direction (n=14) with a pretest score of 0.50 ± 0.08. Each mouse took part in ten trials for up to 4 weeks after BCAO.

Immunohistochemistry

Following MR acquisition, the mice ($n \geq 2$, each group) were put under general anesthesia and retrograde-perfused with ice-cold saline. Whole brains were removed from perfused animals and frozen in n-butanol on dry ice. The frozen brain tissue sections (thickness, 20 μm) were prepared and stored at −70°C before staining. The brain samples were fixed in 4% paraformaldehyde (PFA, 50 ml) in 0.1 M phosphate buffer (0.1 M Na_2HPO_4 /NaH_2PO_4 pH 7.4) for 10 min, and then were washed in buffer. For antigen detection, the samples were stained overnight with rabbit polyclonal antibodies against GFAP (Z0334, Dako), G-CSF

(NBP1-89894, Novous Biologicals), GFP (Z0334A11122, Life Technologies), or NeuN (MAB337, Millipore); all at 1/1000 dilution at 4°C, followed by fluorescein isothiocyanate (FITC)-goat anti-rabbit IgG (1/1000). Vascular endothelia were stained with Cy3-griffonia simplicifolia lectin I (GSL-I, 1/100 dilution), and nucleic acids were stained with Hoechst dye. All histological images were acquired using the same exposure time and gain, using a cellSens system (Olympus USA).

Statistical Tests

We calculated the minimum number of animals required in each group using power analysis to achieve 85% power for a p value of 0.05, or a minimum of n = 2 viable mice in each comparison. We computed the mean and standard error of the mean (SEM) from the average values in each group of animals. We then compared these values using Student t test, one tail; we used the Mann-Whitney test to assess the corner test results.

Acknowledgements

We thank Dr. Sean I. Savitz (University of Texas Houston Medical School, Houston, TX) for demonstration of the corner tests; Dr. Jarek Aronowski (UTHMS, TX) for sharing the hypothermia treatment protocol; Dr. Charng-Ming Liu for synthesizing all sODN and Dr. JS Yang for conducting RT-PCR. This project was supported by NIH grants R01DA029889 and R01EB013768, as well as by a pilot grant from the Boston Area Diabetes Endocrinology Research Center [P30DK057521-14 (J Avruch)] to PKL, NS045776 to the MGH Neuroscience Center]. The MR systems used for this work were funded by NIH Shared Instrumentation Grants (1S10RR025563) awarded to the Athinoula A. Martinos Center for Biomedical Imaging. The B. Wellcome Trust (No.1012722) to HP, State of Florida (09KW-11) to JYW also supported this research.

Non-standard Abbreviations and Acronyms

ADC	Apparent diffusion coefficient
BBB	blood-brain barrier
BCAO	bilateral carotid artery occlusion
DWI	diffusion-weighted imaging
MMP	matrix metalloproteinase
VMD	volume of metabolic disturbance

References cited

1. Talelli P, Ellul J. Are patients with cognitive impairment after stroke at increased risk for developing Alzheimer disease? Archives of neurology. 2004; 61:983. author reply 983. [PubMed: 15210547]
2. Wen Y, et al. Transcriptional regulation of beta-secretase by p25/cdk5 leads to enhanced amyloidogenic processing. Neuron. 2008; 57:680–690. [PubMed: 18341989]
3. Barber RC, et al. Serum granulocyte colony-stimulating factor and Alzheimer's disease. Dement Geriatr Cogn Dis Extra. 2012; 2:353–360. [PubMed: 23012618]
4. Diederich K, et al. The role of granulocyte-colony stimulating factor (G-CSF) in the healthy brain: a characterization of G-CSF-deficient mice. The Journal of neuroscience : the official journal of the Society for Neuroscience. 2009; 29:11572–11581. [PubMed: 19759304]
5. Demetri GD, Griffin JD. Granulocyte colony-stimulating factor and its receptor. Blood. 1991; 78:2791–2808. [PubMed: 1720034]

6. Schneider A, et al. The hematopoietic factor G-CSF is a neuronal ligand that counteracts programmed cell death and drives neurogenesis. The Journal of clinical investigation. 2005; 115:2083–2098. [PubMed: 16007267]
7. Song S, et al. Granulocyte-colony stimulating factor (G-CSF) enhances recovery in mouse model of Parkinson's disease. Neuroscience letters. 2011; 487:153–157. [PubMed: 20951187]
8. Cao XQ, et al. Recombinant human granulocyte colony-stimulating factor protects against MPTP-induced dopaminergic cell death in mice by altering Bcl-2/Bax expression levels. Journal of neurochemistry. 2006; 99:861–867. [PubMed: 17076657]
9. Capoccia BJ, Shepherd RM, Link DC. G-CSF and AMD3100 mobilize monocytes into the blood that stimulate angiogenesis in vivo through a paracrine mechanism. Blood. 2006; 108:2438–2445. [PubMed: 16735597]
10. Gibson CL, Bath PM, Murphy SP. G-CSF reduces infarct volume and improves functional outcome after transient focal cerebral ischemia in mice. Journal of cerebral blood flow and metabolism : official journal of the International Society of Cerebral Blood Flow and Metabolism. 2005; 25:431–439.
11. England TJ, et al. Granulocyte-colony stimulating factor for mobilizing bone marrow stem cells in subacute stroke: the stem cell trial of recovery enhancement after stroke 2 randomized controlled trial. Stroke. 2012; 43:405–411. [PubMed: 22198983]
12. Ringelstein EB, et al. Granulocyte colony-stimulating factor in patients with acute ischemic stroke: results of the AX200 for Ischemic Stroke trial. Stroke. 2013; 44:2681–2687. [PubMed: 23963331]
13. Davis AS, Zhao H, Sun GH, Sapolsky RM, Steinberg GK. Gene therapy using SOD1 protects striatal neurons from experimental stroke. Neuroscience letters. 2007; 411:32–36. [PubMed: 17110031]
14. Liu CH, et al. Noninvasive delivery of gene targeting probes to live brains for transcription MRI. Faseb J. 2008; 22:1193–1203. [PubMed: 18029447]
15. Liu CH, et al. Noninvasive detection of neural progenitor cells in living brains by MRI. FASEB journal : official publication of the Federation of American Societies for Experimental Biology. 2012; 26:1652–1662. [PubMed: 22198388]
16. Henriques A, et al. CNS-targeted viral delivery of G-CSF in an animal model for ALS: improved efficacy and preservation of the neuromuscular unit. Molecular therapy : the journal of the American Society of Gene Therapy. 2011; 19:284–292. [PubMed: 21139572]
17. Liu PK, Grossman RG, Hsu CY, Robertson CS. Ischemic injury and faulty gene transcripts in the brain. Trends Neurosci. 2001; 24:581–588. [PubMed: 11576672]
18. Veldwijk MR, et al. Pseudotyped recombinant adeno-associated viral vectors mediate efficient gene transfer into primary human CD34(+) peripheral blood progenitor cells. Cytotherapy. 2010; 12:107–112. [PubMed: 19929455]
19. Duan D, Yue Y, Yan Z, Engelhardt JF. A new dual-vector approach to enhance recombinant adeno-associated virus-mediated gene expression through intermolecular cis activation. Nature medicine. 2000; 6:595–598.
20. Mandel RJ. CERE-110, an adeno-associated virus-based gene delivery vector expressing human nerve growth factor for the treatment of Alzheimer's disease. Curr Opin Mol Ther. 2010; 12:240–247. [PubMed: 20373268]
21. Theodore S, Cao S, McLean PJ, Standaert DG. Targeted overexpression of human alpha-synuclein triggers microglial activation and an adaptive immune response in a mouse model of Parkinson disease. J Neuropathol Exp Neurol. 2008; 67:1149–1158. [PubMed: 19018246]
22. Whalen MJ, et al. Acute plasmalemma permeability and protracted clearance of injured cells after controlled cortical impact in mice. J Cereb Blood Flow Metab. 2008; 28:490–505. [PubMed: 17713463]
23. Bermpohl D, You Z, Lo EH, Kim HH, Whalen MJ. TNF alpha and Fas mediate tissue damage and functional outcome after traumatic brain injury in mice. J Cereb Blood Flow Metab. 2007; 27:1806–1818. [PubMed: 17406655]
24. Kim F, Bravo PE, Nichol G. What Is the Use of Hypothermia for Neuroprotection After Out-of-Hospital Cardiac Arrest? Stroke. 2015

25. Huang D, Shenoy A, Cui J, Huang W, Liu PK. In situ detection of AP sites and DNA strand breaks bearing 3'-phosphate termini in ischemic mouse brain. Faseb J. 2000; 14:407–417. [PubMed: 10657997]
26. Liu CH, Huang S, Kim YR, Rosen BR, Liu PK. Forebrain ischemia-reperfusion simulating cardiac arrest in mice induces edema and DNA fragmentation in the brain. Mol Imaging. 2007; 6:156–170. [PubMed: 17532882]
27. Kida K, et al. Sodium sulfide prevents water diffusion abnormality in the brain and improves long term outcome after cardiac arrest in mice. Resuscitation. 2012; 83:1292–1297. [PubMed: 22370005]
28. Minamishima S, et al. Inhaled nitric oxide improves outcomes after successful cardiopulmonary resuscitation in mice. Circulation. 2011; 124:1645–1653. [PubMed: 21931083]
29. Dijkhuizen RM, et al. Functional magnetic resonance imaging of reorganization in rat brain after stroke. Proceedings of the National Academy of Sciences of the United States of America. 2001; 98:12766–12771. [PubMed: 11606760]
30. Li X, et al. Chronic behavioral testing after focal ischemia in the mouse: functional recovery and the effects of gender. Exp Neurol. 2004; 187:94–104. [PubMed: 15081592]
31. Yli-Hankala A, Edmonds HL Jr, Jiang YD, Higham HE, Zhang PY. Outcome effects of different protective hypothermia levels during cardiac arrest in rats. Acta Anaesthesiol Scand. 1997; 41:511–515. [PubMed: 9150781]
32. Liu CH, et al. Diffusion-weighted magnetic resonance imaging reversal by gene knockdown of matrix metalloproteinase-9 activities in live animal brains. J Neurosci. 2009; 29:3508–3517. [PubMed: 19295156]
33. Pardridge WM, Boado RJ, Kang YS. Vector-mediated delivery of a polyamide ("peptide") nucleic acid analogue through the blood-brain barrier in vivo. Proc Natl Acad Sci U S A. 1995; 92:5592–5596. [PubMed: 7777554]
34. Liu PK, et al. Suppression of ischemia-induced fos expression and AP-1 activity by an antisense oligodeoxynucleotide to c-fos mRNA. Ann Neurol. 1994; 36:566–576. [PubMed: 7944289]
35. Gibson CL, Jones NC, Prior MJ, Bath PM, Murphy SP. G-CSF suppresses edema formation and reduces interleukin-1beta expression after cerebral ischemia in mice. Journal of neuropathology and experimental neurology. 2005; 64:763–769. [PubMed: 16141785]
36. Liu CH, Ren J, Liu CM, Liu PK. Intracellular gene transcription factor protein-guided MRI by DNA aptamers in vivo. FASEB journal : official publication of the Federation of American Societies for Experimental Biology. 2014; 28:464–473. [PubMed: 24115049]
37. Schaar KL, Brenneman MM, Savitz SI. Functional assessments in the rodent stroke model. Exp Transl Stroke Med. 2010; 2:13. [PubMed: 20642841]
38. Zhang L, et al. A test for detecting long-term sensorimotor dysfunction in the mouse after focal cerebral ischemia. Journal of neuroscience methods. 2002; 117:207–214. [PubMed: 12100987]
39. Liu CH, et al. MRI reveals differential effects of amphetamine exposure on neuroglia in vivo. FASEB journal : official publication of the Federation of American Societies for Experimental Biology. 2013; 27:712–724. [PubMed: 23150521]
40. Liu CH, et al. DNA-based MRI probes for Specific Detection of Chronic Exposure to Amphetamine in Living Brains. J Neurosci. 2009; 29:10663–10670. [PubMed: 19710318]
41. Liu CH, et al. MR contrast probes that trace gene transcripts for cerebral ischemia in live animals. Faseb J. 2007; 21:3004–3015. [PubMed: 17478745]

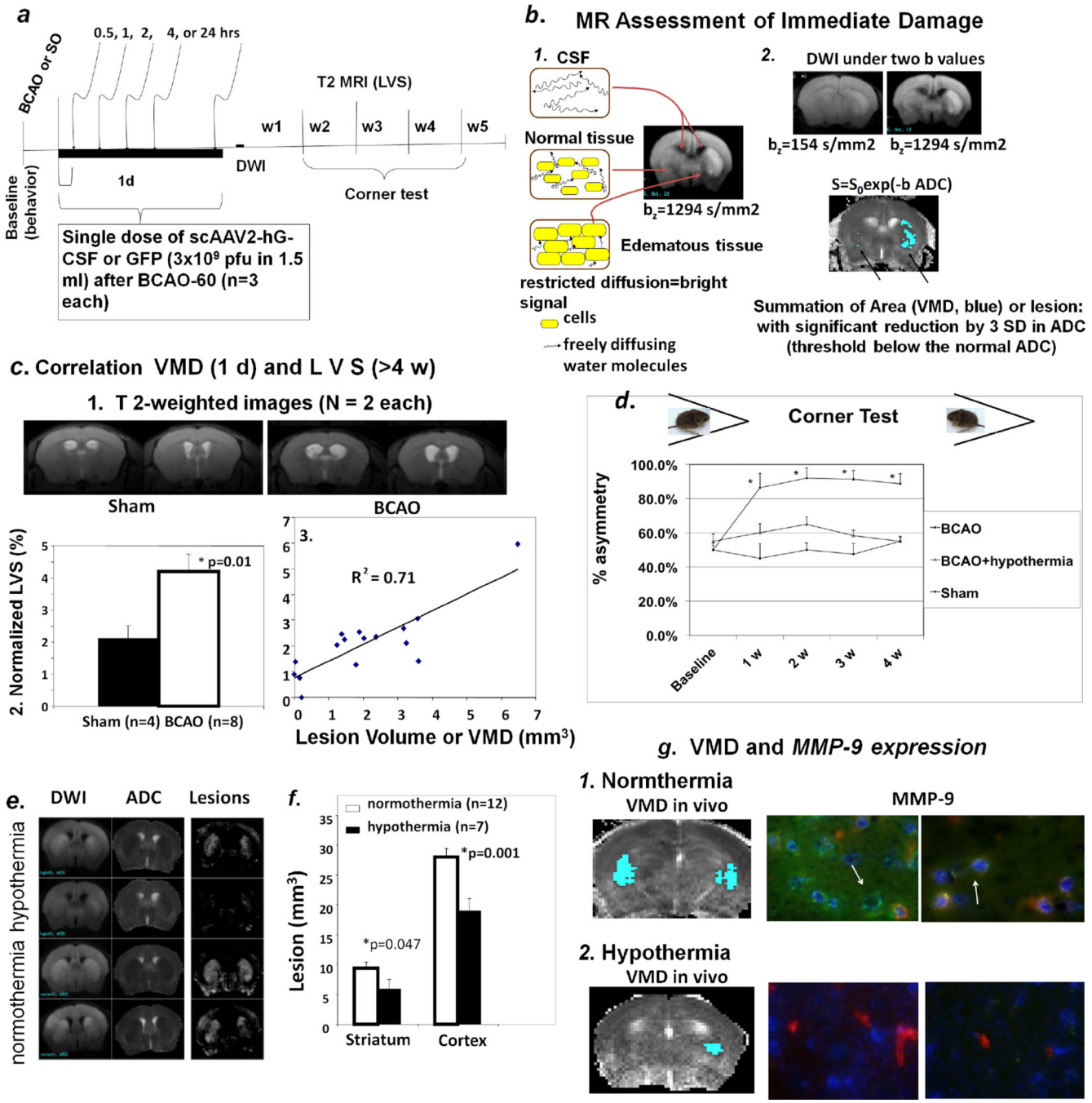

Figure 1.

Panel *a*. Protocol for longitudinal monitoring of brain repair in vivo using MRI in mice with BCAO or sham operation. We made weekly measurements (up to 10 weeks, w10): for cerebral atrophy (ventriculomegaly) without MR-CA at w4 or w5, expression of scAAV2-CMV-hG-CSF, baseline MRI using SPION-Ran studies. The protocol can be extended to 24 weeks in some studies for leakage of the BBB using Gd-DATA. Panel *b*. Abnormal DWI is obvious at high b values; DWIs before and after BCAO are shown (frame 1). High-lighted areas showing significant below-threshold rADC after BCAO-60 represent regions of

interest (ROI) for calculating the volume of metabolic disturbance (VMD, summation of all ROI of five MR slices of 1 mm each) as the lesion size (mm^3). The results of BCAO-60, including abnormal water diffusion in the cerebrospinal fluid (CSF) in normal tissue as well as tissue with edema are illustrated, as detected by MRI (frame 2). Panel *c*-1. Representative T2-weighted images (caudal view). Enlarged lateral ventricles show cerebral atrophy without visible abnormal T2 MRI from mice at weeks 4 and 5 following sham operation and BCAO (one of five MR images from each mouse). Panel c-2. Normalized lateral ventricular size (LVS). We measured ventriculomegaly (n = 16) as normalized lateral ventricular size (LVS, or by size ratio of lateral ventricle to corresponding brain volumes in percent, %). Panel c-3. Scatter plot of LSV and VDM from mice before (n = 4) and after (n = 12) BCAO-60. The scatter plot shows the correlation between LVS (%) at w4–w5 post BCAO and lesion volume (VMD) in the same mice. Panel *d*. Corner test results of BCAO mice (normothermia, n = 8 survivors of 32; hypothermia, n = 6; sham-operation, n = 4) when facing a 30° corner. BCAO mice without treatment showed significant asymmetric turning (~90%) beginning one week after the procedure and persisting for at least four weeks. Mice with treatment (BCAO + hypothermia) exhibited behavior not significant differently from that seen in the sham-operated mice. Panels *e*–*h*. Validations of noninvasive measurements. Hypothermia treatment reversed DWI and rADC (e) as well as VMD (f). The expression of MMP-9 antigen one day post-BCAO in postmortem samples (*g*, arrows point to vascular MMP-9, green) validates brain lesion reduction with hypothermia treatment, shown here as normothermia (*g1*) vs. hypothermia (*g2*). (Endothelia = red; Nuclei = Hoechst stain).

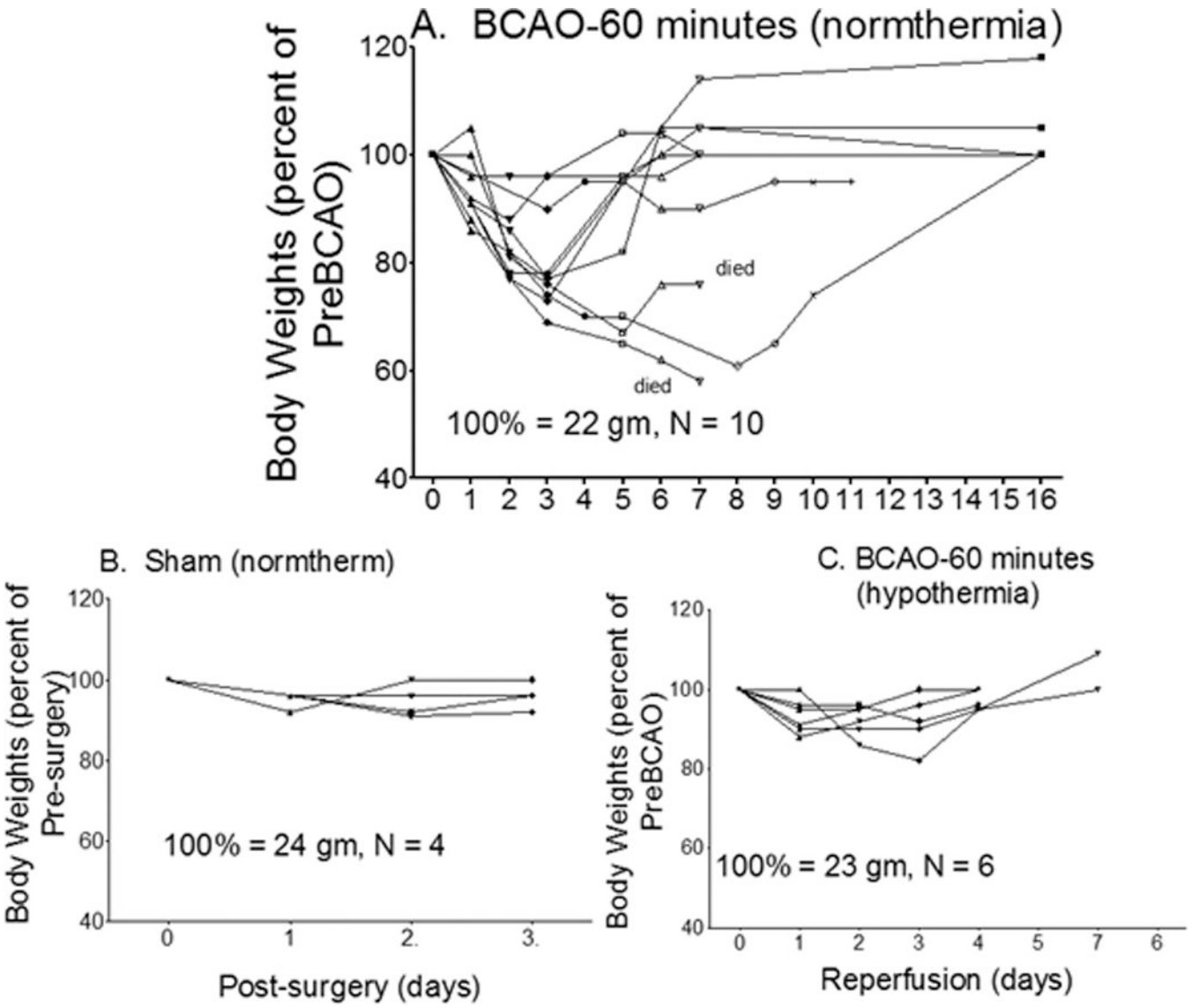

Figure 2.

Changes in body weight before and after BCAO, with and without hypothermia treatment. Body weights of mice after BCAO were measured and recorded daily for at least 7 days after BCAO-60.

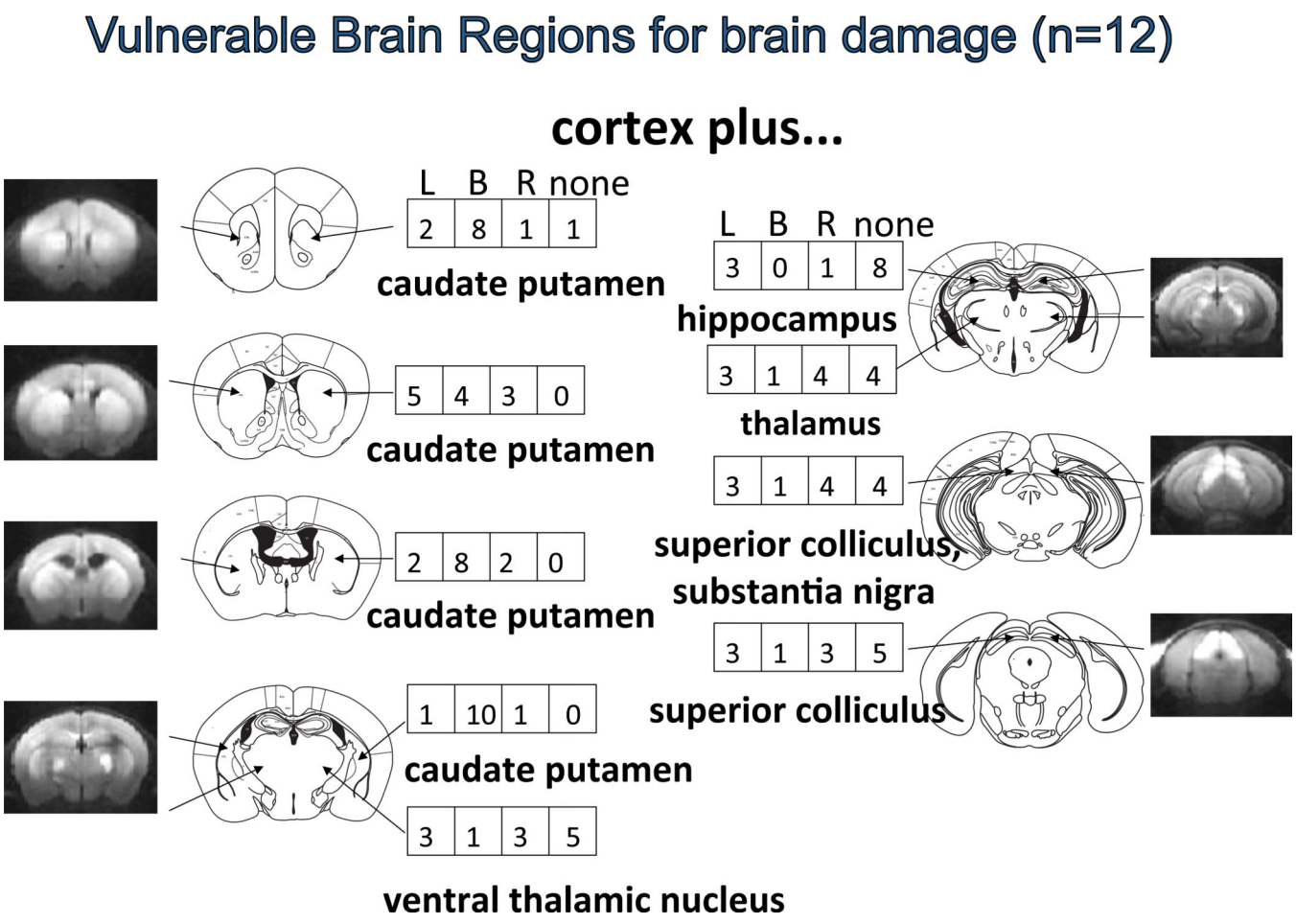

Figure 3.

Summary of potential brain damage (or BBB disruption) measured by MRI at the second peak of DWI or 1 to 2 days after BCAO-60 in C57black6 mice. The number in the box indicates the number of mice exhibiting lesion in the left (L), right (R) both (B) hemispheres [reconstructed from[32]]. The presence of a lesion in the superior colliculus or optic tectum (midbrain) indicates BCAO effects that extend beyond the forebrain; mouse cardiac arrest-resuscitation models also show hyperintense DWI (hDWI) in similar ROI[27,28].

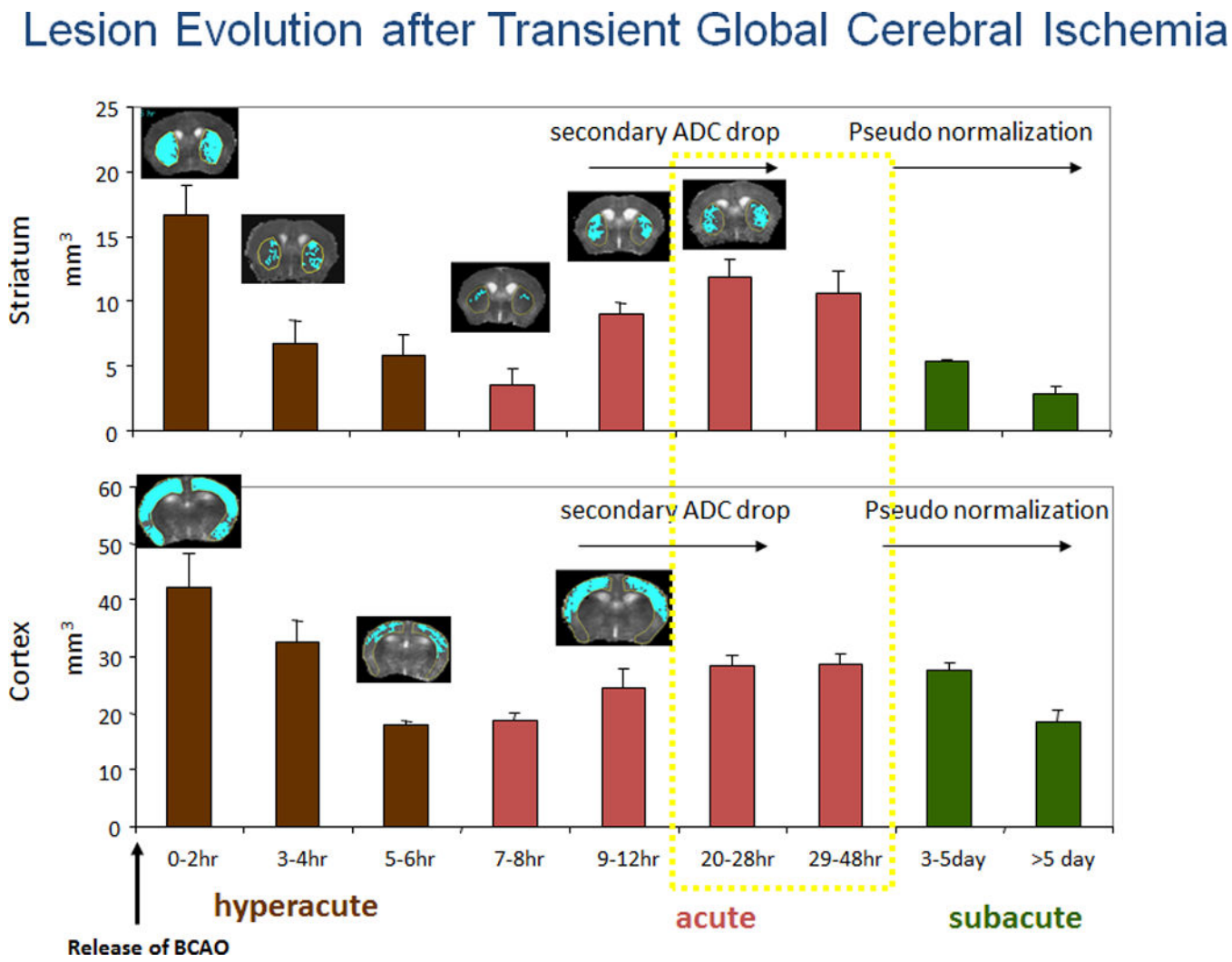

Figure 4.

The time course followed for applying the AAV-CMV vector. Early brain lesions estimated by rADC below the threshold values (see Fig 1c). The tthreshold of ADC in normal mice (n = 6 at different dates and different litters of mice) was established using power analysis after BCAO at normal temperature (Each data point after BAO was obtained from at least n ≥ 4, Data adapted from our previous publication)[32].

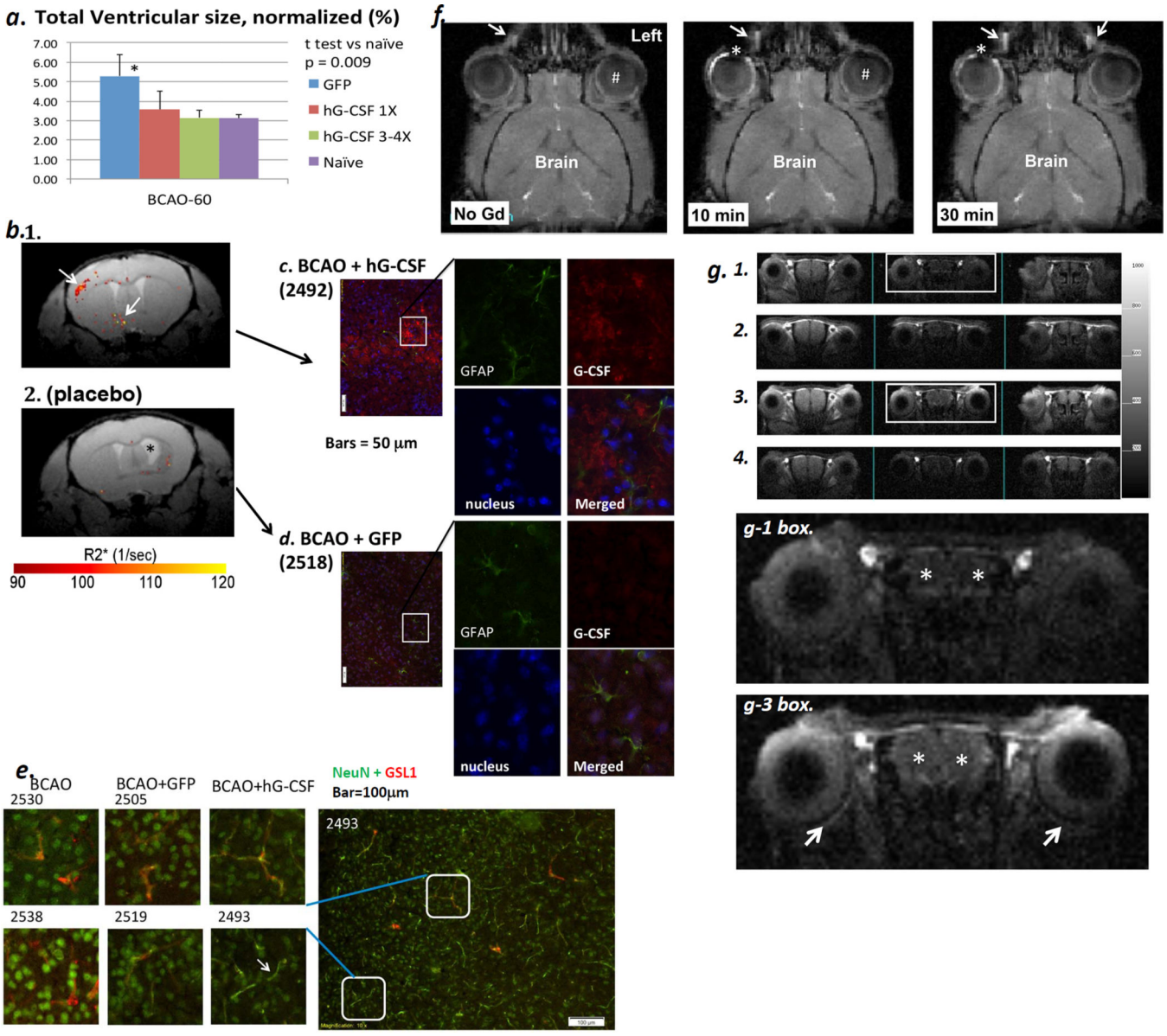

Figure 5.

Panel *a*. Significant reduction in cerebral atrophy (measured during the 4th week after BCAO, purple bar) in the scAAV2-CMV-hG-CSF treatment groups with multiple doses (green bar, n = 5 survivors of 5) compared to the placebo group (blue bar, n = 7 survivors of 28) or BCAO+ single dose hG-CSF (red bar, n = 5 survivors of 8). We validated the expression of hG-CSF antigen using immunohistochemistry in the 11th week (Panels *c* & *d*). Panel *b*. A unique ROI (arrow) using SPION-AS-hG-CSF one week after the final scAAV2-CMV-hG-CSF treatment (the 3rd week). Panel *b1*. The ROI in delta R2* maps from both the multiple treatment (n = 5) and placebo (n = 4 survivors of 16, Panel *b*2) groups of mice. Panels *c & d*. hG-CSF expression in the proximity of the ROI identified in vivo (*b*1), with no expression found in the placebo group (*b2 & d*). Mice with BCAO only did not show elevated hG-CSF expression (n = 2 survivors of 8, data not shown). Panel *e*. NeuN

expression in small blood vessels (Cy3-GSL I) in mice with AAV2-CMV-hG-CSF (BCAO +hG-CSF, n = 3) bar = 100 μm. NeuN expression (Cy2, arrow) occurs mostly in the neuronal nuclei of control and placebo groups (BCAO, n = 2 survivors of 8; BCAO+GFP, n = 4 survivors of 16). Panel *f*. T1-weighted MRI of mice (n=4) before and after application of eye drops containing non-targetng MR-CA (Gd-DTPA, 500 mM in 10 μl Magnevist, Scherling, Berlin, Germany) to the conjunctival sac; the distribution of MR-CA is shown in the same mouse. Arrow: the naso-lacrimal canal, #: the vitrous chamber; asterisk: lens. Panel *g*. The distribution of targeted MR-CA (Gd-nestin) in longitudinal MR acquisition (n = 2). T1-weighted MRI was acquired before (*g*1), 10 min (*g*2), 180 min (*g*3) and 41 hr (*g*4) after application of Gd-nestin (50 μg Gd-NA and 30 pmol biotin-sODN-nestin per 2 μl per mouse to one eye) in mice with BCAO-60. Arrows: chorid of the retina; * both hemispheres of the brain. Biotinylated sODN-nestin binds to NeutrAvidin (NA) on SPION or Gd and the MR-CA targets Nestin mRNA of percytes of neovessels after BCAO-60[14,15].

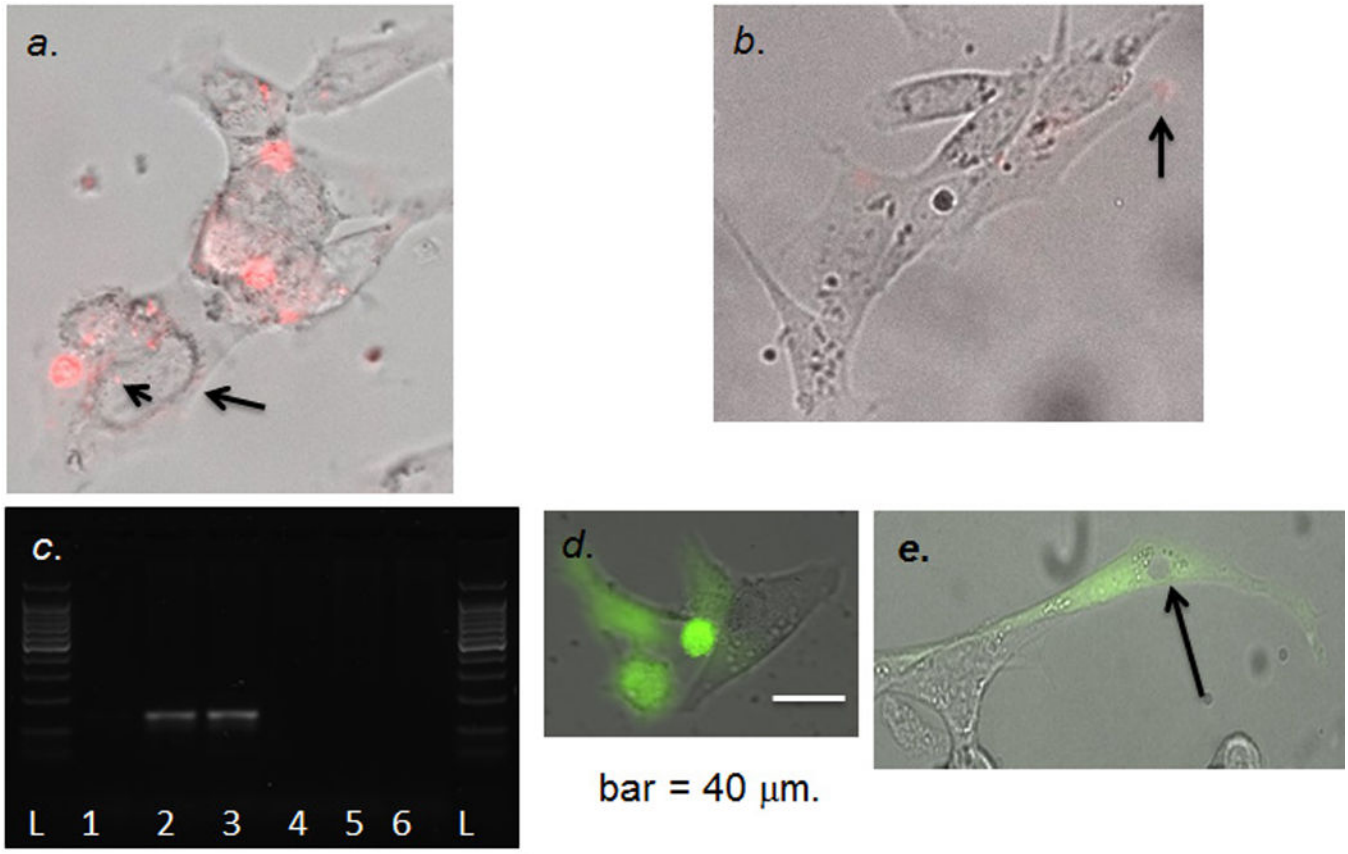

Figure 6.

Panel *a*. hG-CSF cDNA/mRNA expression in PC-12 cells. We transfected Cy3-sODN-AS-hG-CSF to detect hG-CSF mRNA in cells transfected with pCMV-hG-CSF; we observed signal in the nucleus (arrowhead) and peri-nucleus (arrow). Panel *b*. Few Cy3-sODN-AS-hG-CSF (arrow) retention in the cells transfected with pCMV-GFP. Panel *c*. Validation of hG-CSF mRNA expression from transfected PC-12 cells (pCMV-hG-CSF [lanes 1–3] or pCMV-GFP [lanes 4–6] at 3 (lanes1, 4), 6 (Lanes 2, 5) or 8 (lanes 3, 6) hours after transfection. Isolated RNA was treated with DNase before reverse transcription. Panel *d*. Living cells with GFP expression (Z-stack photograph, cellSens, time-lapse optical microscopy, Olympus IX83) >3 hours after transfection with pCMV-GFP. Panel *e*. Stable pCMV-GFP DNA in vivo for 72 hours. We isolated total DNA from PC-12 at 72 hours (Panel d); we then transfected PC-12 again and detected GFP expression at 24 hours after transfection. GFP is in the cytoplasm but there is no nuclear GFP (arrow).